Inorg. Chem. **2009**, *48*, 3215−3227

Ruthenium Phthalocyanine-Bipyridyl Dyads as Sensitizers for Dye-Sensitized Solar Cells: Dye Coverage versus Molecular Efficiency

Tristan Rawling,[†] Christine Austin,[†] Florian Buchholz,[†] Stephen B. Colbran,[‡] and Andrew M. McDonagh*[,†]

Institute for Nanoscale Technology, University of Technology Sydney, Sydney NSW 2007, Australia, and School of Chemistry, The University of New South Wales, Sydney NSW 2052, Australia

Received October 30, 2008

The application of ruthenium phthalocyanine complexes as sensitizing dyes in dye-sensitized solar cells (DSCs) is explored. Four monomeric complexes are reported which vary in peripheral substitution and axial ligand anchoring groups. Sensitizing dyes containing two ruthenium centers are also presented. These dyads, which contain ruthenium phthalocyanine and bipyridyl chromophores, were prepared using a protection/deprotection strategy that allows for convenient purification. DSCs fabricated using the phthalocyanine complexes and dyads were less efficient than those incorporating a standard DSC dye. However, on the basis of the number of molecules bound to the TiO_2 electrode surfaces, several of the new complexes were more efficient at photocurrent generation. The results highlight the importance of molecular size, and thus the dye coverage of the electrode surface in the design of new sensitizing dyes.

Introduction

Dye-sensitized solar cells (DSCs) have been the focus of sustained research as alternatives to silicon-based photovoltaic devices. DSCs can be flexible and semi-transparent allowing them to be incorporated into building materials and other devices. Many aspects of DSCs have been investigated to improve their efficiency, but a factor attracting significant attention is the sensitizing dye.[1,2] Since the discovery of the landmark bis(bipyridyl)ruthenium sensitizing dyes *cis*-$[Ru(H_2dcbpy)_2(X)_2]$ (where H_2dcbpy = 4,4′-dicarboxylic acid-2,2′-bipyridine and X = Cl^-, Br^-, I^-, CN^-, or NCS^-) over a decade ago[3] only a handful of superior dyes have been prepared, and all of these have been polypyridyl ruthenium(II) species.[4−6] Research into new sensitizing dyes is increasingly focused on preparing compounds that can absorb photons with wavelengths of 600−900 nm where the solar photon flux[7] is greatest within the visible region.

Ruthenium phthalocyanine (PcRu) complexes are attractive as sensitizing dyes as they possess intense and tunable absorptions in the region of ∼650 nm,[8] as well as a reversible ring-based oxidation.[9] Several examples of PcRu-sensitized DSCs exist in which the dye is attached to the TiO_2 via axial ligands[10−12] or through anchoring groups on the macrocycle periphery.[13] Promising results were obtained with [{1,4,8,-11,15,18,22,25-Me_8Pc}Ru(3,4-pyridinedicarboxylic acid)]

* To whom correspondence should be addressed. E-mail: andrew.mcdonagh@uts.edu.au.
† University of Technology Sydney.
‡ The University of New South Wales.

(1) Robertson, N. *Angew. Chem., Int. Ed.* **2006**, *45*, 2338.
(2) Robertson, N. *Angew. Chem., Int. Ed.* **2008**, *47*, 1012.
(3) Nazeeruddin, M. K.; Kay, A.; Rodicio, I.; Humphry-Baker, R.; Mueller, E.; Liska, P.; Vlachopoulos, N.; Grätzel, M. *J. Am. Chem. Soc.* **1993**, *115*, 6382.
(4) Wang, P.; Zakeeruddin, S. M.; Moser, J. E.; Humphry-Baker, R.; Comte, P.; Aranyos, V.; Hagfeldt, A.; Nazeeruddin, M. K.; Graetzel, M. *Adv. Mater.* **2004**, *16*, 1806.
(5) Grätzel, M. *J. Photochem. Photobiol., C* **2003**, *4*, 145.
(6) Nazeeruddin, M. K.; Pechy, P.; Renouard, T.; Zakeeruddin, S. M.; Humphry-Baker, R.; Comte, P.; Liska, P.; Cevey, L.; Costa, E.; Shklover, V.; Spiccia, L.; Deacon, G. B.; Bignozzi, C. A.; Graetzel, M. *J. Am. Chem. Soc.* **2001**, *123*, 1613.
(7) American Society for Testing and Materials, ASTM G 159-98, 2000, 14.04
(8) Rawling, T.; McDonagh, A. *Coord. Chem. Rev.* **2007**, *251*, 1128.
(9) Rawling, T.; Xiao, H.; Lee, S.-T.; Colbran, S. B.; McDonagh, A. M. *Inorg. Chem.* **2007**, *46*, 2805.
(10) Nazeeruddin, M. K.; Humphry-Baker, R.; Grätzel, M.; Murrer, B. A. *Chem. Commun.* **1998**, 719.
(11) Yanagisawa, M.; Korodi, F.; He, J.; Sun, L.; Sundstrom, V.; Akermark, B. *J. Porphyrins Phthalocyanines* **2002**, *6*, 217.
(12) O'Regan, B. C.; Lopez-Duarte, I.; Martinez-Diaz, M. V.; Forneli, A.; Albero, J.; Morandeira, A.; Palomares, E.; Torres, T.; Durrant, J. R. *J. Am. Chem. Soc.* **2008**, *130*, 2906.
(13) Yanagisawa, M.; Korodi, F.; Bergquist, J.; Holmberg, A.; Hagfeldt, A.; Akermark, B.; Sun, L. *J. Porphyrins Phthalocyanines* **2004**, *8*, 1228.

10.1021/ic802087n CCC: $40.75
Published on Web 03/11/2009

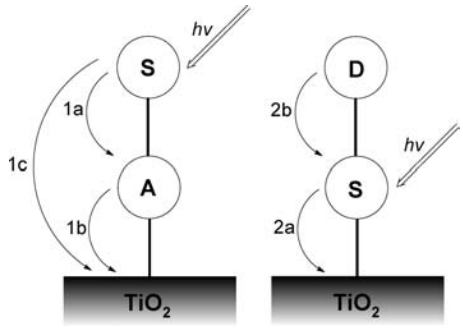

Figure 1. Electron transfer processes in acceptor-sensitizer (left) and sensitizer-donor (right) complexes anchored on TiO_2.

which returned photocurrent yields of over 50% in the region 600−700 nm.[10] Other metallophthalocyanines, in particular zinc complexes,[14−17] have also been successfully used as sensitizers in DSCs.

One design strategy for improved dyes involves maximizing the distance between the positive "hole" created after electron injection and the TiO_2 surface, thus creating a long-lived charge separated state by reducing the rate of electron recombination. The result is a lowering of the titania quasi-Fermi level and a gain in the cell potential.[18] Sensitizers designed using this strategy can generally be classified as either acceptor-sensitizer or sensitizer-donor complexes (see Figure 1). Acceptor-sensitizer complexes operate via stepwise electron injection. The first step is absorption of a photon by the sensitizer, and the resulting excited electron may be transferred to the acceptor (process 1a). The reduced acceptor may then inject the electron into the TiO_2 conduction band (process 1b). Photocurrent may also be generated by remote electron injection from the sensitizer excited-state directly into the TiO_2 conduction band (process 1c). In sensitizer-donor complexes the excited sensitizer electron is injected directly into the TiO_2 (process 2a). Transfer of an electron from the donor to the oxidized sensitizer returns the sensitizer to its ground state (process 2b), with the positive "hole" shifted away from the TiO_2 surface.

The acceptor-sensitizer complexes [Rh(H_2dcbpy)$_2$-(BL)-Ru(bpy)$_2$] and [Rh(H_2dcbpy)$_2$-(BL)-Ru(bmp)$_2$] (bmp = 4,7-dimethyl-1,10-phenanthroline and BL = 1,2-bis[4-(4′-methyl-2,2′-bipyridyl)]ethane) were found to undergo remote electron injection and stepwise electron injection when utilized in DSCs.[19] Recombination was slower compared to a model mononuclear compound, and the poor photovoltaic performance was assigned to poor charge injection yields. Stepwise electron injection was also observed in a mixed-valence Co^{III}/Fe^{II} complex; however, the low absorption coefficient of the complex lead to poor photovoltaic performance.[20] The first examples of donor-sensitizer complexes used in DSCs were [Ru(H_2dcbpy)$_2$(4-CH_3, 4′-CH_2-X-2,2′-bipyridine)]$^{2+}$ (X = phenothiazine derivatives).[21,22] In these dyads the pendant phenothiazine acts as an electron donor, with hole transport away from the TiO_2 surface leading to longer lived charge separated states. The reduced recombination rates lead to an increase in cell potential. A similar result was obtained using bis(terpyridine) ruthenium complexes bearing triarylamine donor components.[18] Attachment of cyclodextrins to a tris(bipyridyl) ruthenium core lead to an improvement of all DSC performance measures.[23] Hole hopping was observed from the oxidized tris(bipyridyl) ruthenium core to the cyclodextrin component. Regeneration of the complex was facilitated by the ability of cyclodextrin to bind iodine and triiodide.

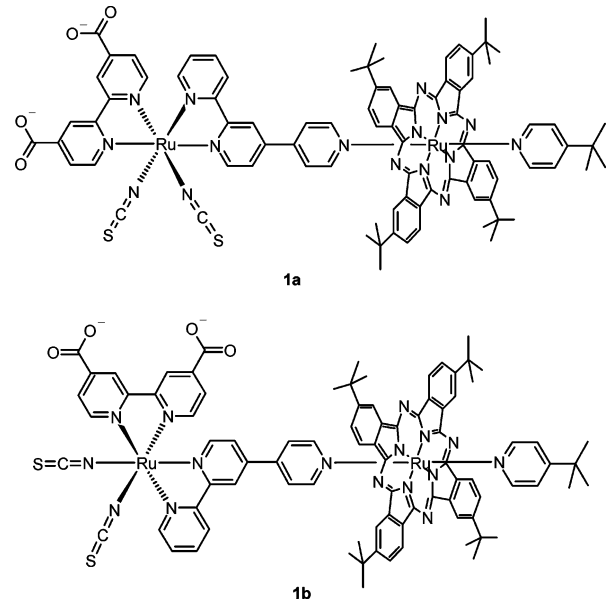

Figure 2. Ruthenium dyads, **1a** and **1b** that incorporate bis(bipyridyl)ruthenium(II) and ruthenium phthalocyanine chromophores.

We have synthesized new ruthenium phthalocyanine-bipyridyl ruthenium dyads as sensitizers for DSCs. We report here on the photovoltaic performance of several ruthenium phthalocyanine sensitizing dyes including the new dyads that incorporate bis(bipyridyl)ruthenium(II) (BpyRu) and ruthenium phthalocyanine chromophores (Figure 2). We sought to combine the excellent electron injection efficiency of BpyRu complexes with the intense light absorption of PcRu complexes. The complementary absorption spectra typically displayed by the two chromophores permits the use of most of the visible spectrum for photocurrent generation. The

(14) Cid, J.-J.; Yum, J.-H.; Jang, S.-R.; Nazeeruddin, M. K.; Martinez-Ferrero, E.; Palomares, E.; Ko, J.; Grätzel, M.; Torres, T. *Angew. Chem., Int. Ed.* **2007**, *46*, 8358.
(15) Reddy, P. Y.; Giribabu, L.; Lyness, C.; Snaith, H. J.; Vijaykumar, C.; Chandrasekharam, M.; Lakshmikantam, M.; Yum, J.-H.; Kalyanasundaram, K.; Grätzel, M.; Nazeeruddin, M. K. *Angew. Chem., Int. Ed.* **2007**, *46*, 373.
(16) Chen, Y.; Zeng, Z.; Li, C.; Wang, W.; Wang, X.; Zhang, B. *New J. Chem.* **2005**, *29*, 773.
(17) Yum, J.-H.; Jang, S.-R.; Humphry-Baker, R.; Grätzel, M.; Cid, J.-J.; Torres, T.; Nazeeruddin, M. K. *Langmuir* **2008**, *24*, 5636.
(18) Bonhote, P.; Moser, J.-E.; Humphry-Baker, R.; Vlachopoulos, N.; Zakeeruddin, S. M.; Walder, L.; Graetzel, M. *J. Am. Chem. Soc.* **1999**, *121*, 1324.
(19) Kleverlaan, C. J.; Indelli, M. T.; Bignozzi, C. A.; Pavanin, L.; Scandola, F.; Hasselman, G. M.; Meyer, G. J. *J. Am. Chem. Soc.* **2000**, *122*, 2840.
(20) Bernhardt, P. V.; Boschloo, G. K.; Bozoglian, F.; Hagfeldt, A.; Martinez, M.; Sienra, B. *New J. Chem.* **2008**, *32*, 705.
(21) Argazzi, R.; Bignozzi, C. A.; Heimer, T. A.; Castellano, F. N.; Meyer, G. J. *J. Am. Chem. Soc.* **1995**, *117*, 11815.
(22) Argazzi, R.; Bignozzi, C. A.; Heimer, T. A.; Castellano, F. N.; Meyer, G. J. *J. Phys. Chem. B* **1997**, *101*, 2591.
(23) Faiz, J.; Philippopoulos, A. I.; Kontos, A. G.; Falaras, P.; Pikramenou, Z. *Adv. Funct. Mater.* **2007**, *17*, 54.

Scheme 1. Synthesis of the Ruthenium Phthalocyanine Sensitizing Complexes

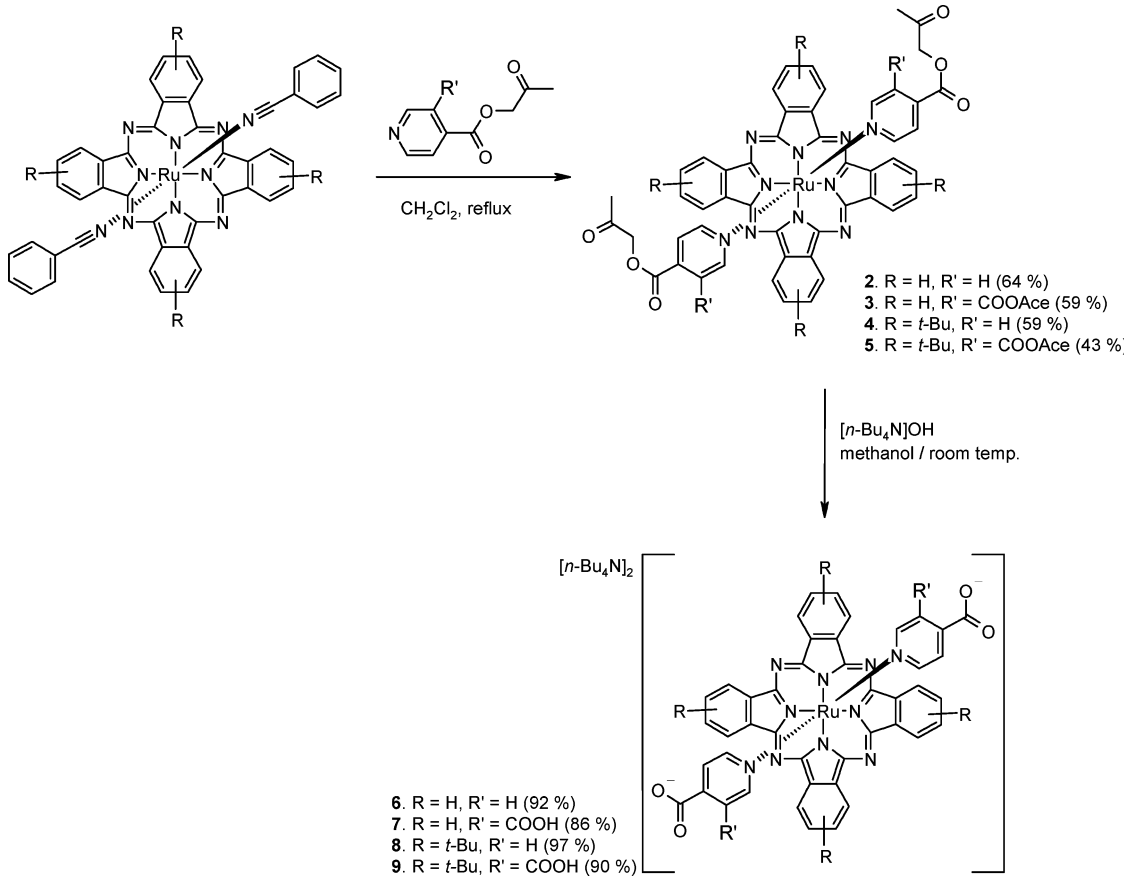

BpyRu-PcRu dyads presented in this work consist of two chromophores, each of which may act as an electron donor and acceptor. These complexes may therefore display dual modes of operation, functioning as both acceptor-sensitizer and sensitizer-donor complexes in DSCs. Importantly, we find that although the new dyads are capable of generating significant photocurrents, the number of these large molecules that adsorb to the DSC electrode surface severely limits the overall cell performance.

Results and Discussion

Synthesis. All of the sensitizing complexes prepared in this work contain carboxyl functional groups to anchor the dyes to TiO_2 electrode surfaces. A synthetic strategy using esters to protect the carboxyl groups during synthesis was adopted to enable rapid and effective purification of the dyes using silica gel column chromatography.[24,25] The ester-protected complexes can be reacted with tetrabutylammonium (TBA) hydroxide to yield the desired TBA salts of the complexes, which are preferred to the fully protonated complexes as they offer greater solubility and have been shown to improve the performance of DSCs.[26]

The syntheses of the PcRu complexes **6**−**9** is shown in Scheme 1. The ligands 4-pyCOOAce and 3,4-py(COOAce)$_2$ were prepared in moderate yields by reaction of the corresponding carboxylic acids with hydroxyacetone via the Steglich esterification.[27] Replacement of the labile benzonitrile ligands of [PcRu(PhCN)$_2$] and [{(*t*-Bu)$_4$Pc}Ru(PhCN)$_2$] afforded the acetolyl protected intermediate complexes **2**−**5**. We note that the peripherally substituted complexes **4** and **5** consist of four positional isomers,[28] which were not separated. Deprotection of the intermediate acetolyl complexes using TBAOH was rapid and complete.

The methods used to prepare the bis(bipyridyl)ruthenium complexes **10**−**12** and dyads **1** and **13** are shown in Scheme 2. Acetolyl protecting groups were unstable under these reaction conditions and so an *iso*-butyl ester protected ligand, *bis*(2-methylpropyl)-2,2′-bipyridine-4,4′-dicarboxylate (*i*Bu$_2$-dcbpy), was used. The branched-chain *iso*-butyl groups also imparted good solubility to the resultant complexes. Complex **10** was prepared in relatively low yield by adapting literature procedures[29−31] using butanol as solvent. Using DMF as solvent resulted in even lower yields, possibly because of hydrolysis of the ester groups by dimethylamine formed from

(24) Patterson, B. T.; Keene, F. R. *Aust. J. Chem.* **1998**, *51*, 999.
(25) Rawling, T.; Buchholz, F.; McDonagh, A. M. *Aust. J. Chem.* **2008**, *61*, 405.
(26) Nazeeruddin, M. K.; Zakeeruddin, S. M.; Humphry-Baker, R.; Jirousek, M.; Liska, P.; Vlachopoulos, N.; Shklover, V.; Fischer, C.-H.; Grätzel, M. *Inorg. Chem.* **1999**, *38*, 6298.
(27) Kundu, B. *Tetrahedron Lett.* **1992**, *33*, 3193.
(28) Knecht, S.; Polley, R.; Hanack, M. *Appl. Organomet. Chem.* **1996**, *10*, 649.
(29) Wang, P.; Humphry-Baker, R.; Moser, J. E.; Zakeeruddin, S. M.; Graetzel, M. *Chem. Mater.* **2004**, *16*, 3246.
(30) Jang, S.-R.; Lee, C.; Choi, H.; Ko, J. J.; Lee, J.; Vittal, R.; Kim, K.-J. *Chem. Mater.* **2006**, *18*, 5604.
(31) Nazeeruddin, M. K.; Zakeeruddin, S. M.; Lagref, J. J.; Liska, P.; Comte, P.; Barolo, C.; Viscardi, G.; Schenk, K.; Graetzel, M. *Coord. Chem. Rev.* **2004**, *248*, 1317.

Scheme 2. Synthesis of **1a** and **1b**[a]

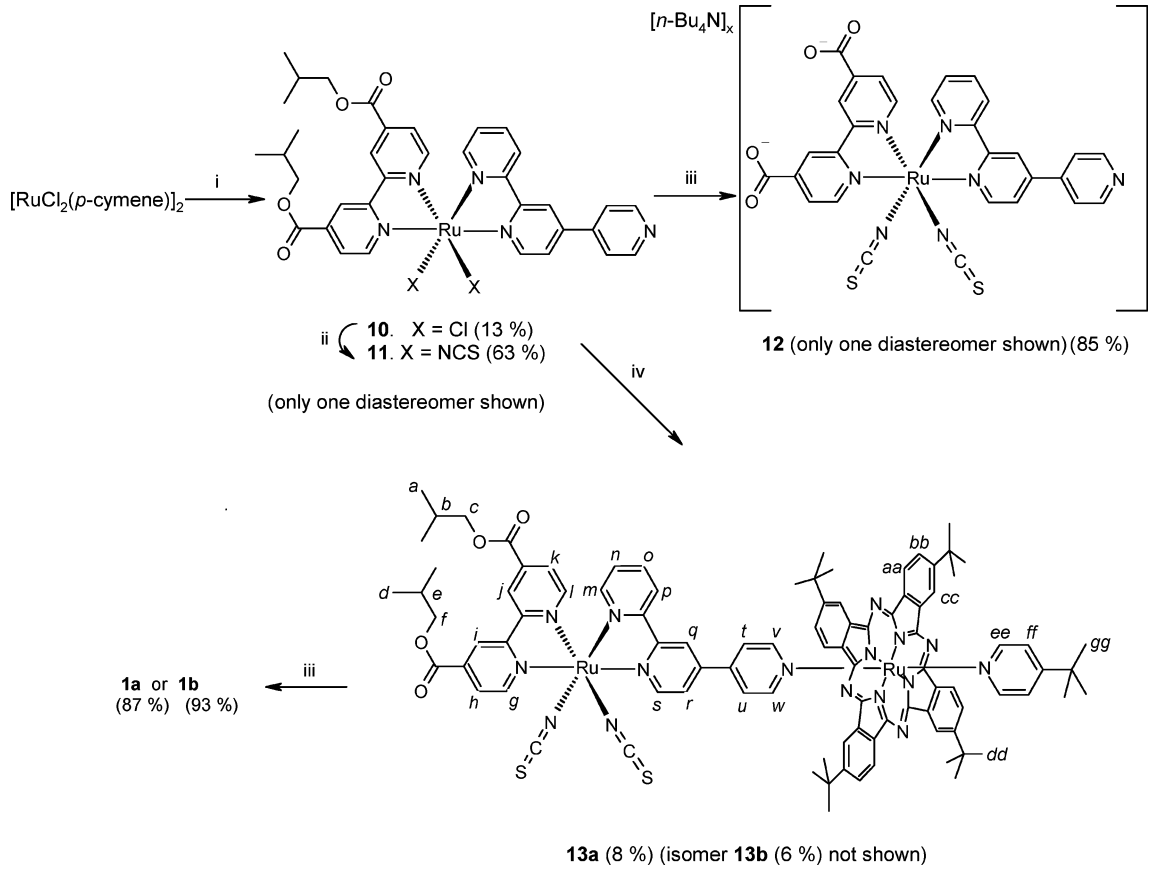

[a] Reaction conditions: (i) *i*Bu$_2$dcbpy, butanol, 85 °C, 1.5 h then 2,2′:4′,4″-terpyridine, reflux, 3.5 h; (ii) [NH$_4$]NCS, ethanol, reflux, 3h; (iii) 1M TBAOH in methanol, 20 min. (note: full deprotonation of the carboxyl groups was not observed: x ≈ 0.5); (iv) [{(*t*-Bu)$_4$Pc}Ru(PhCN)$_2$], 4-*tert*-butylpyridine, dichloromethane, reflux, 3.5 h.

decomposition of DMF.[32] We believe the low yields of **10** result from displacement of a chloro ligand in the product by the pendant pyridyl of the 2,2′:4′,4″-terpyridine ligand. This type of reaction is known to proceed at temperatures lower than those used during the formation of **10**.[33−35] In addition, significant quantities of the *trans*-isomer of **10** were isolated from the reaction mixture. Complex **11** was prepared by replacement of the chloro ligands of **10** with thiocyanato ligands, which may bond through either the nitrogen or the sulfur atom. The fully N-bonded linkage isomer was desired as, based on the example of [Bu$_4$N]$_2$[Ru(4-carboxy-4-carboxylate-2,2′-bipyridine) $_2$(NCS)$_2$] (known commonly as N719), it should be the more efficient DSC sensitizer.[3] The linkage isomers were separated by silica gel chromatography, and the fully N-bound isomer **11** was identified by ^{1}H NMR spectroscopy (see below). Upon deprotection of **11** with TBAOH, the TBA salt of the dianion did not precipitate. However, careful addition of nitric acid precipitated the product with 0.5 TBA cations per complex molecule, which corresponds to a 1:1 mixture of the monodeprotonated and fully protonated **12**. Each of the bipyridyl complexes **10**, **11**, and **12** was isolated as a mixture of two diastereomers in which the 4′,4″-bipyridyl moiety is *trans* to either the Cl/NCS coligand or the bipyridyl ligand.

In the synthesis of the axially unsymmetrically substituted phthalocyanine complexes, **13a** and **13b**, both axial ligands (i.e., **11** and 4-*tert*-butylpyridine) were added to [{(*t*-Bu)$_4$Pc}Ru(PhCN)$_2$] at the same time and the reaction therefore resulted in a mixture of four complexes, the desired axially unsymmetrical complexes **13a** and **13b** together with two axially symmetrical complexes. Thus, the yields of **13a** and **13b** were relatively low. Importantly, the two isomers **13a** and **13b** could be separated, not only from the axially symmetrical complexes, but also from each other using silica gel column chromatography. De-esterification of **13a** and **13b** with TBAOH afforded the dyads **1a** and **1b** in excellent yields.

^{1}H NMR Spectroscopy. The ^{1}H NMR spectra of the peripherally *tert*-butyl substituted phthalocyanine complexes **4**−**5**, **8**−**9**, and the unsubstituted complexes **2**−**3**, **6**−**7** are typical for these classes of phthalocyanines[8] (see Supporting Information together with a discussion of the spectra of **10**−**13**).

Proton assignments were made for the dyads **13a** and **13b** using ^{1}H−^{1}H COSY NMR experiments (see the Supporting

(32) Perrin, D. D.; Armarego, W. L. F. *Purification of Laboratory Chemicals*, 3rd ed.; Pergamon Press: Oxford, 1988.
(33) Du, M.; Ge, X.-J.; Liu, H.; Bu, X.-H. *J. Mol. Struct.* **2002**, *610*, 207.
(34) Toma, S. H.; Uemi, M.; Nikolaou, S.; Tomazela, D. M.; Eberlin, M. N.; Toma, H. E. *Inorg. Chem.* **2004**, *43*, 3521.
(35) Liu, Y.; Song, S.-H.; Chen, Y.; Zhao, Y.-L.; Yang, Y.-W. *Chem. Commun.* **2005**, 1702.

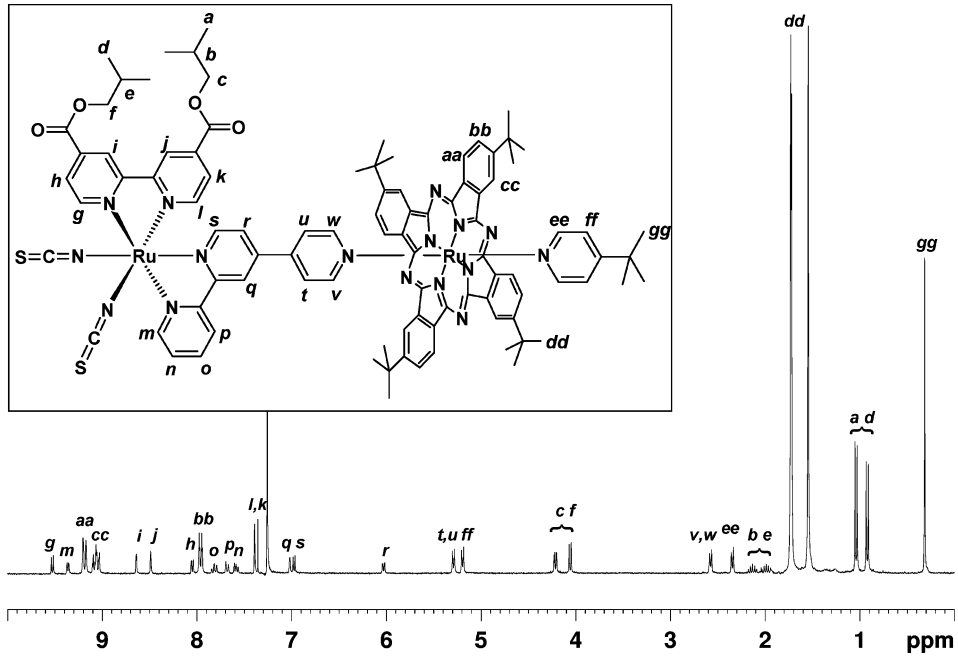

Figure 3. ^{1}H NMR spectrum of **13b** in $CDCl_3$ with peak assignments.

Information). Figure 3 shows the ^{1}H NMR spectrum of **13b** together with the assignment of each of the proton signals. Coordination of the electron-withdrawing bipyridyl unit shifts the phthalocyanine ring proton resonances to higher frequency compared to those for **4**−**5**, and **8**−**9**. Protons on the 4′,4″-bipyridyl moiety of the bridging terpyridyl ligand and those of 4-*tert*-butylpyridine are significantly shielded by the phthalocyanine ring current, with the extent of the shielding decreasing as the distance from the ring increases. Peaks assigned to protons *v*, *w* and *t*, *u* are further downfield relative to *ee* and *ff* because of the electron withdrawing effect of the bipyridyl unit. Protons on rings that are in the vicinity of the thiocyanato ligands are deshielded,[26,36,37] with *g* and *m* experiencing the greatest deshielding. In **13a** (see Scheme 2), *m* − *p* are no longer in the vicinity of a thiocyanato ligand, and all shift to lower frequency compared to **13b**. Protons *s*, *r*, and *q* are deshielded by a thiocyanato ligand and shift to higher frequency relative to **13b**, particularly *s* which shifts by 2.18 ppm. The spectra of **1a** and **1b** are similar to those of the corresponding protected complexes. The only resonances that shift significantly are those *meta* to the carboxylate group (*g* and *l*) which shift to lower frequency by ∼ 0.4 ppm.

UV−**vis spectroscopy.** The electronic spectra of the phthalocyanine complexes **2**−**9** are dominated by intense Q- and Soret bands (see Figure 4). The Soret bands, which arise mainly from the ring-based HOMO-1 to LUMO transitions,[38] show little variation in energy across the series and appear between 313−317 nm (ε_{max} = 91000−117000 M^{-1} cm^{-1}).

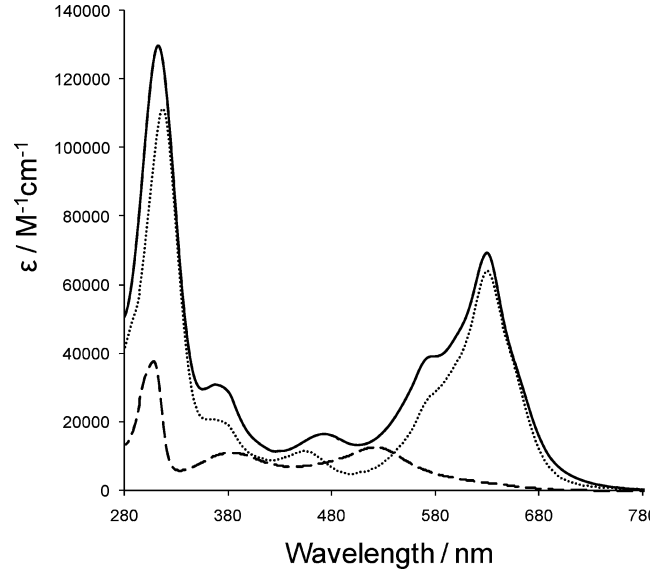

Figure 4. UV−visible spectra of **9** (dotted line), **12** (dashed line), and **1b** (solid line) in dichloromethane.

The less intense Q-bands (ε_{max} = 52000−70000 M^{-1} cm^{-1}), which arise from ring-centered HOMO to LUMO transitions,[38] are observed with λ_{max} in the range 623−645 nm. The spectra of **2**−**5** also contain absorption bands at ∼470 nm (ε_{max} = 11000−14000 M^{-1} cm^{-1}). A similar absorption band has been found in the electronic spectra of complexes of the type [PcRuL$_2$] (L = azanaphthalenes) and was attributed to a metal-to-ligand charge transfer (MLCT) transition.[39] Upon conversion of **3** and **5** to their TBA salts these absorption bands undergo hypsochromic shifts of 1420 and 1190 cm^{-1}, respectively. These bands are not evident in the spectra of **6** and **8** but may be hidden by the intense Soret bands. The Q-bands of **2**−**5** also undergo a small

(36) Wolfbauer, G.; Bond, A. M.; MacFarlane, D. R. *Inorg. Chem.* **1999**, *38*, 3836.
(37) Shklover, V.; Nazeeruddin, M. K.; Zakeeruddin, S. M.; Barbe, C.; Kay, A.; Haibach, T.; Steurer, W.; Hermann, R.; Nissen, H. U.; Grätzel, M. *Chem. Mater.* **1997**, *9*, 430.
(38) Stillman, M. J.; Nyokong, T. In *Phthalocyanines: Properties and Applications*; Leznoff, C. C., Lever, A. B. P., Eds.; VCH: New York, 1989; p 133.
(39) Hanack, M.; Kang, Y. G. *Chem. Ber.* **1991**, *124*, 1607.

Table 1. Electrochemical Data for Redox Processes[a,b]

process	$E_{1/2}$, V vs Fc^+/Fc (ΔE_p, V)						
	6	**7**	**8**	**9**	**12**[c]	**1a**	**1b**
d						1.29 (0.12)	1.30 (0.12)
d	0.90 (0.13)	0.99 (0.18)	0.96 (0.11)	0.91 (0.10)			
Pc^{1-}, Pc^0	0.81 (0.14)	0.79 (0.14)	0.67 (0.18)	0.72 (0.11)		0.81 (0.07)	0.83 (0.07)
d						0.71 (0.08)	0.73 (0.08)
d					0.67[e]		
d						0.37 (0.08)	0.39 (0.09)
Ru^{II}, Ru^{III}					0.37 (0.13)	0.31[e]	0.36[e]
Pc^{2-}, Pc^{1-}	0.15 (0.09)	0.16 (0.08)	0.05 (0.08)	0.05 (0.09)		0.16 (0.10)	0.17 (0.11)
dcbpy reduction					−1.89 (0.08)	−1.77 (0.09)	−1.75 (0.09)
Pc^{2-}, Pc^{3-}	−1.75 (0.10)	−1.74 (0.10)	−1.82 (0.09)	−1.84 (0.11)		−1.89 (0.08)	−1.84 (0.08)

[a] In dichloromethane−$[Bu_4N][PF_6]$ (0.1 M) at scan rate 100 mV s^{-1}. [b] One-electron processes. [c] In 9:1 dichloromethane: dimethylformamide. [d] Unassigned. [e] Anodic peak for irreversible process.

hypsochromic shift upon conversion to the corresponding TBA salts.

Complex **10** shows two absorption bands in the visible region at 587 and 433 nm, arising from metal-to-ligand charge transfer (MLCT) transitions.[3,40] Replacement of chloro ligands with thiocyanato ligands in bis(bipyridyl)ruthenium(II) complexes leads to a hypsochromic shift of the MLCT band.[26,37] With **11**, these absorption bands are hypsochromically shifted by 890 and 1000 cm^{-1}, respectively, compared to **10**. Deprotection of **11** to give **12** causes a further hypsochromic shift. The spectra of **10** and **11** also display two strong absorption bands at ∼307 and 318 nm, which are assigned to ligand-centered π-π^* transitions[3,40] of the terpyridyl and bipyridyl ligands respectively. Complex **12** (see Figure 4) shows only one absorption in the UV region, a result of a hypsochromic shift of the bipyridyl-based transition caused by the carboxylate groups, which leads to overlapping π-π^* absorption bands. A similar hypsochromic shift of this band was reported upon deprotonation of $[Ru(H_2dcbpy)(dmbpy)(NSC)_2]$ (dmbyp = 4,4′-dimethyl-2,2′-bipyridine).[31]

The electronic spectra of the dyads **13a**, **13b**, **1a**, and **1b** (see Figure 4) are dominated by the intense phthalocyanine absorption bands. Importantly, the Q-bands appear at 630 nm, the region of maximum solar photon flux.[7] The Soret bands of **13a** and **13b** appear at ∼317 nm and have a very high molar extinction coefficient (ε_{max} = ∼143 000 M^{-1} cm^{-1}) because of the underlying BpyRu center, which also has an absorption band at 318 nm. In **1a** and **1b** the intensity of the Soret band decreases by ∼14 000 M^{-1} cm^{-1} as the underlying BpyRu absorption band shifts to higher energy following de-esterification; a similar shift is observed in the spectrum of **12**.

Electrochemistry. The thermodynamics for the first oxidation and first reduction processes of sensitizing dyes are critical to DSC performance. Information about these processes was obtained using cyclic voltammetry (Table 1). The cyclic voltammograms of the PcRu complexes **6**−**9** show minor variation across the series which is attributed to the different phthalocyanine ring substituents. Each of these complexes displays one reduction and three oxidation processes (see Figure 5 and the Supporting Information). The

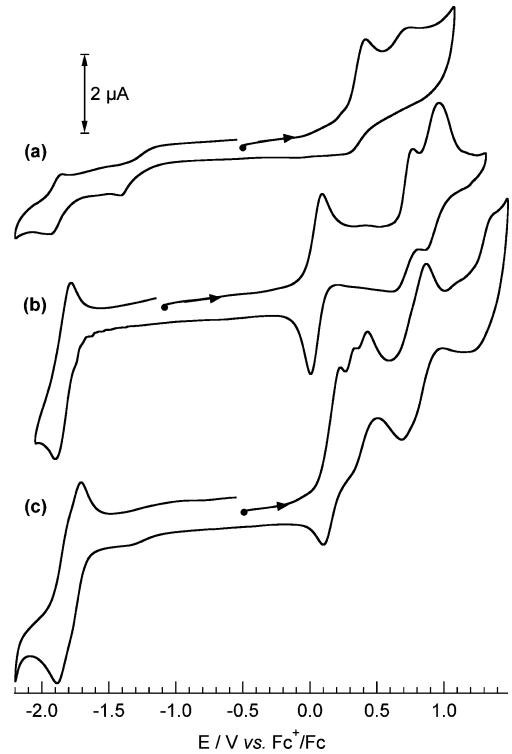

Figure 5. Cyclic voltammograms of **12** (a; in 9:1 dichloromethane: dimethylformamide solution), **9** (b), and **1b** (c) in dichloromethane solution with 0.1 M $[Bu_4N][PF_6]$ electrolyte; glassy carbon minidisk (0.5 mm) working electrode, scan rate = 100 mV s^{-1}.

reversible one-electron reductions involve the $[Pc^{2-}Ru^{II}]/[Pc^{3-}Ru^{II}]^-$ couple with the $E_{1/2}$ values similar to those reported for the macrocycle-based reduction of other peripherally unsubstituted[41−44] and tetra-*tert*-butyl substituted[9] PcRu complexes. The first two oxidations are both macrocycle-centered one-electron processes corresponding to the $[Pc^{2-}Ru^{II}]/[Pc^{-}Ru^{II}]^+$ and $[Pc^{-}Ru^{II}]^+/[Pc^{0}Ru^{II}]^{2+}$ couples, and the potentials are typical for these types of complexes.[9,41,43,45] The second oxidations of **6**−**9** are quasi-reversible. A third irreversible oxidation was observed. In general, the data show that the peripheral *tert*-butyl groups increase the electron

(40) Lagref, J. J.; Nazeeruddin, M. K.; Graetzel, M. *Inorg. Chim. Acta* **2008**, *361*, 735.
(41) Weidemann, M.; Hueckstaedt, H.; Homborg, H. *Z. Anorg. Allg. Chem.* **1998**, *624*, 846.
(42) Sievertsen, S.; Weidemann, M.; Huckstadt, H.; Homborg, H. *J. Porphyrins Phthalocyanines* **1997**, *1*, 379.
(43) Durr, K.; Hanack, M. *J. Porphyrins Phthalocyanines* **1999**, *3*, 224.
(44) Ebadi, M.; Alexiou, C.; Lever, A. B. P. *Can. J. Chem* **2001**, *79*, 992.
(45) Dolphin, D.; James, B. R.; Murray, A. J.; Thornback, J. R. *Can. J. Chem.* **1980**, *58*, 1125.

density at the macrocycle while the 4-pyCOO$^-$ and 3,4-py(COOH)COO$^-$ axial ligands exert similar influence to each other.

The electrochemical properties of **12** are similar to those reported for *cis*-[Ru(dcbpyH$_2$)$_2$(NCS)$_2$] (known commonly as N3).[3,46−48] A single reversible one-electron reduction (see Figure 5b) assigned to the reduction of the dcbpy ligand is observed at −1.89 V (vs Fc/Fc$^+$). The first oxidation, assigned to the Ru^{II}/Ru^{III} couple, is quasi-reversible and occurs at a similar potential to that of N3[3,47] and related ruthenium heteroleptic[29,31,40] complexes.

The dyads **1a** and **1b** each display six oxidation and two reduction processes (see Figure 5 and the Supporting Information). Interestingly, the redox processes associated with **1b** occur at potentials 10−50 mV more positive than those of **1a**. The two reductions are reversible, one-electron processes separated by ∼100 mV. The first is attributed to reduction of the dcbpy ligand, and the second to reduction of the PcRu ring (see the spectroelectrochemistry discussion below). The first oxidations of **1a** and **1b** are reversible one-electron oxidations of the PcRu rings, which are again assigned from spectroelectrochemical data (see below). The potentials of these processes are more positive than those of **8** and **9** because of the electron withdrawing BpyRu unit. The second oxidations at ∼0.33 V are irreversible one-electron processes and are assigned to the bipyridyl Ru^{II}/Ru^{III} couple.[49]

Spectroelectrochemistry. Spectroelectrochemical experiments were used to further probe the electrochemical behavior of the phthalocyanine-containing dyes. Panels a and b of Figure 6 show the spectroscopic changes that occur upon oxidation of complex **9**. During the first oxidation (Figure 6a) the Q-band was replaced by a broad absorption at 544 nm, and the Soret band diminished slightly in intensity. These changes are consistent with a one-electron oxidation of the phthalocyanine ring to yield the reasonably stable π-cation radical.[9,45,50,51] During the second oxidation (Figure 6b) the band at 544 nm arising from the π-cation radical disappears, and the Soret band weakens significantly while a broad absorption at 399 nm appears. These changes indicate that the second oxidation is also a macrocycle-based process and forms the [Pc^{0}Ru^{II}] species.[9] Decomposition of the complex occurred during the third oxidation and so this process was unable to be investigated.

During the reductive electrolysis of **12** (Figure 7a) the MLCT bands undergo hypsochromic shifts and decrease in intensity. The changes observed are analogous to those observed during the reduction of N3 at a platinum electrode,[46] and result from the redox-linked deprotonation of the carboxyl groups accompanied by evolution of molecular hydrogen. The site of reduction observed using this technique is different compared to CV because of the different working electrodes used (Pt vs glassy carbon).[46] Figure 7b shows the development of the absorption spectrum of **12** as the oxidation proceeded. The changes are analogous to those reported for the ruthenium-based oxidation of N3 in aceto-

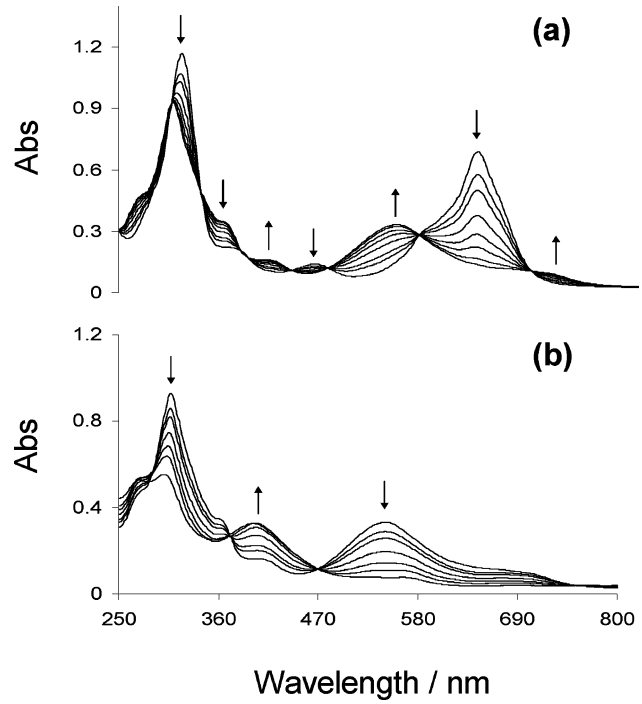

Figure 6. UV−vis spectra recorded during the oxidative electrolyses of **9** in dichloromethane (0.1 M [*n*-Bu$_4$N][PF$_6$]); (a) first oxidation process at 0.15 V, (b) second oxidation process at 0.82 V.

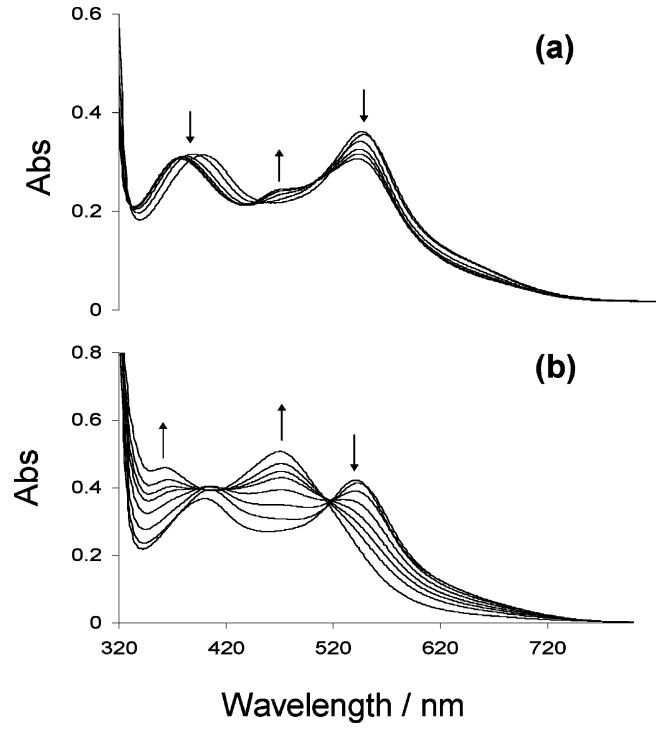

Figure 7. UV−vis spectra recorded during the reduction (a) and first oxidation (b) of **12** in dichloromethane/DMF (0.1 M/0.2 [*n*-Bu$_4$N][PF$_6$] for the oxidation/reduction) using a Pt electrode.

(46) Wolfbauer, G.; Bond, A. M.; Deacon, G. B.; MacFarlane, D. R.; Spiccia, L. *J. Am. Chem. Soc.* **2000**, *122*, 130.
(47) Bond, A. M.; Deacon, G. B.; Howitt, J.; MacFarlane, D. R.; Spiccia, L.; Wolfbauer, G. *J. Electrochem. Soc.* **1999**, *146*, 648.
(48) Cecchet, F.; Gioacchini, A. M.; Marcaccio, M.; Paolucci, F.; Roffia, S.; Alebbi, M.; Bignozzi, C. A. *J. Phys. Chem. B* **2002**, *106*, 3926.
(49) Argazzi, R.; Bignozzi, C. A.; Hasselmann, G. M.; Meyer, G. J. *Inorg. Chem.* **1998**, *37*, 4533.
(50) Rodriguez-Morgade, M. S.; Planells, M.; Torres, T.; Ballester, P.; Palomares, E. *J. Mater. Chem.* **2008**, *18*, 176.
(51) Nyokong, T. *Polyhedron* **1993**, *12*, 375.

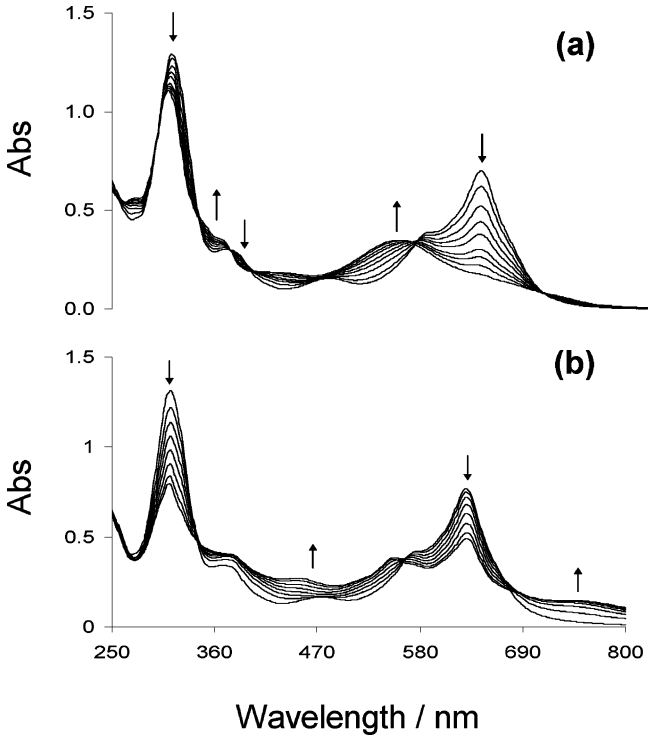

Figure 8. UV−vis spectra recorded during the oxidative electrolyses of **1b** in dichloromethane (0.1 M [*n*-Bu_4N][PF_6]): (a) first oxidation process at 0.26 V; (b) second reduction process at −1.95 V.

nitrile or ethanol.[48] The oxidation of N3 was reported to be solvent dependent, and a clear consensus on the oxidation product identity is not apparent;[36,48,52] however, the changes shown in Figure 7b indicate that upon oxidation of **12** both of the thiocyanato ligands are converted to cyanato ligands (generated by oxidation of thiocyanate) or are replaced by solvent, as suggested by others.[36,48,52]

Figure 8a shows the changes in the UV−vis spectra of **1b** as the first oxidation proceeded. The changes are analogous to those observed for the first oxidation of **9** and are attributed to a one-electron oxidation of the phthalocyanine ring. At potentials beyond the second and third oxidations all the absorption bands decreased uniformly as decomposition of the complex occurs. Spectroelectrochemistry was useful in assigning the two almost overlapping reduction processes of the dyads. During the first reduction of **1b** no major changes in the UV−vis spectrum were observed. This is consistent with electron addition to the dcbpy ligand of the BpyRu center noting that the absorption bands of the BpyRu moiety are obscured by the intense PcRu absorption bands. Figure 8b shows that at potentials beyond the second reduction of **1b** the Q-band diminishes in intensity and a second Q-band appears at 553 nm. The Soret band also diminishes in intensity. These changes are consistent with a one-electron reduction of the phthalocyanine ring[9] and therefore the second reduction corresponds to the $[Pc^{2-}Ru^{II}]/[Pc^{3-}Ru^{II}]^-$ couple.

The electrochemical potentials of the **1a** and **1b** give an indication[53] of their electronic structure, and analysis of the data indicates that both hole hopping and stepwise electron injection are energetically feasible. Hole hopping in the case of the dyads constitutes electron transfer from the phthalocyanine ring-based HOMO to the SOMO or "hole" of the BpyRu component (located mainly on the ruthenium center[54]) after electron injection into the TiO_2 conduction band ($E_{1/2}$ (Pc^{2-}/Pc^-) = ∼0.16 V and ($E_{1/2}$ (Ru^{II}/Ru^{III}) = ∼0.38 V). Stepwise electron injection involves transfer of a photoexcited electron from the phthalocyanine ring-based LUMO into the LUMO of the BpyRu component, which is located on the bipyridyl[54] ligand. In both dyads, this should be energetically feasible as $E_{1/2}$ (Pc^{3-}/Pc^{2-}) = − 1.89 V and $E_{1/2}$ ($dcbpy^-$/dcbpy) = − 1.77 V.

TiO_2 Surface Adsorption. The number of surface-adsorbed sensitizing dye molecules on the TiO_2 electrodes of DSCs is an important factor in photocurrent generation and therefore overall cell performance although it is most often not reported in DSC characterization data. It has been generally estimated using UV−vis spectroscopy,[3,55−59] although photoelectron spectroscopy[60] has also been used. We have developed a sensitive method to determine the amount of surface-adsorbed dye molecules using inductively coupled plasma mass-spectrometry (ICP MS). ICP MS has remarkably low detection limits; concentrations in the range of ng/mL to mg/mL can be measured.

Sensitizing dyes were adsorbed onto TiO_2 electrodes (identical to those used in DSC experiments), which were then thoroughly washed and dried. The TiO_2/adsorbed dye component was removed and weighed. The dyes were desorbed from the TiO_2 surface following the procedure of Dabestani et al.[55] The addition of 1 M tetramethylammonium hydroxide (TMAOH) in ethanol/water to the dye-coated TiO_2 caused an immediate decoloration of the TiO_2 which was then left for 2 h to ensure complete desorption. The concentration of ^{101}Ru in the resulting solution was measured using ICP MS. Surface adsorption data are presented in Table 2. ^{101}Ru concentrations were in the μg/mL range, well within the detection limits of the instrument. N719 had the greatest number of surface-adsorbed molecules, followed closely by **12**. The dyads had approximately half the number of surface-adsorbed molecules compared to **12**, indicating that inclusion of the PcRu component significantly increases steric bulk

(52) Hansen, G.; Gervang, B.; Lund, T. *Inorg. Chem.* **2003**, *42*, 5545.
(53) *Inorganic Electronic Structure and Spectroscopy, Volume II: Applications and Case Studies*; Solomon, E. I., Lever, A. B. P., Eds.; Wiley: New York, 1999.
(54) Zhang, X.; Zhang, J.-J.; Xia, Y.-Y. *J. Photochem. Photobiol., A* **2007**, *185*, 283.
(55) Dabestani, R.; Bard, A. J.; Campion, A.; Fox, M. A.; Mallouk, T. E.; Webber, S. E.; White, J. M. *J. Phys. Chem.* **1988**, *92*, 1872.
(56) Rochford, J.; Chu, D.; Hagfeldt, A.; Galoppini, E. *J. Am. Chem. Soc.* **2007**, *129*, 4655.
(57) Zukalova, M.; Prochazka, J.; Zukal, A.; Yum, J. H.; Kavan, L. *Inorg. Chim. Acta* **2008**, *361*, 656.
(58) Kusama, H.; Kurashige, M.; Sayama, K.; Yanagida, M.; Sugihara, H. *J. Photochem. Photobiol., A* **2007**, *189*, 100.
(59) Altobello, S.; Bignozzi, C. A.; Caramori, S.; Larramona, G.; Quici, S.; Marzanni, G.; Lakhmiri, R. *J. Photochem. Photobiol., A* **2004**, *166*, 91.
(60) Westermark, K.; Rensmo, H.; Siegbahn, H.; Keis, K.; Hagfeldt, A.; Ojamaee, L.; Persson, P. *J. Phys. Chem. B* **2002**, *106*, 10102.

Table 2. Photovoltaic Performance Data for DSCs Prepared with the Sensitizing Complexes Investigated in This Work[a,b]

dye	J_{sc} (mA/cm^2)	V_{oc} (mV)	P_{max} (μW/cm^2)	fill factor	η (%)	dye coverage (μmol of dye/g of TiO_2)
6[b]	0.30 ± 0.07	148 ± 7	19 ± 4	0.43 ± 0.14	0.038 ± 0.008	12.6 ± 0.5
7[b]	1.28 ± 0.07	231 ± 1	121 ± 6	0.41 ± 0.03	0.24 ± 0.01	22.8 ± 0.9
8[b]	0.37 ± 0.02	166 ± 4	27 ± 3	0.44 ± 0.05	0.054 ± 0.006	6.97 ± 0.16
9[b]	1.23 ± 0.02	232 ± 9	124 ± 9	0.44 ± 0.02	0.25 ± 0.02	14.6 ± 1.2
9[c]	0.35 ± 0.01	403 ± 6	87 ± 2	0.61 ± 0.02	0.17 ± 0.01	
12[b]	2.12 ± 0.10	316 ± 12	383 ± 8	0.50 ± 0.03	0.77 ± 0.02	31.8 ± 0.2
1a[b]	1.13 ± 0.03	275 ± 1	144 ± 5	0.46 ± 0.02	0.29 ± 0.01	14.5 ± 0.1
1b[b]	1.33 ± 0.02	273 ± 7	169 ± 7	0.47 ± 0.03	0.34 ± 0.01	17.4 ± 0.9
1b[c]	0.05 ± 0.01	308 ± 7	5 ± 1	0.32 ± 0.08	0.010 ± 0.002	
N719[b]	2.74 ± 0.13	412 ± 18	541 ± 37	0.48 ± 0.04	1.01 ± 0.07	37.3 ± 2.4
N719[c]	1.50 ± 0.03	632 ± 4	558 ± 17	0.59 ± 0.02	1.11 ± 0.03	

[a] Cells illuminated with a halogen lamp at 500 Wm^{-2}. [b] Electrolyte: 0.05 M I_2 and 0.7 M LiI in 3-methoxypropionitrile. [c] Electrolyte: 0.05 M I_2, 0.7 M LiI and 0.5 M 4-*tert*-butylpyridine in 3-methoxypropionitrile.

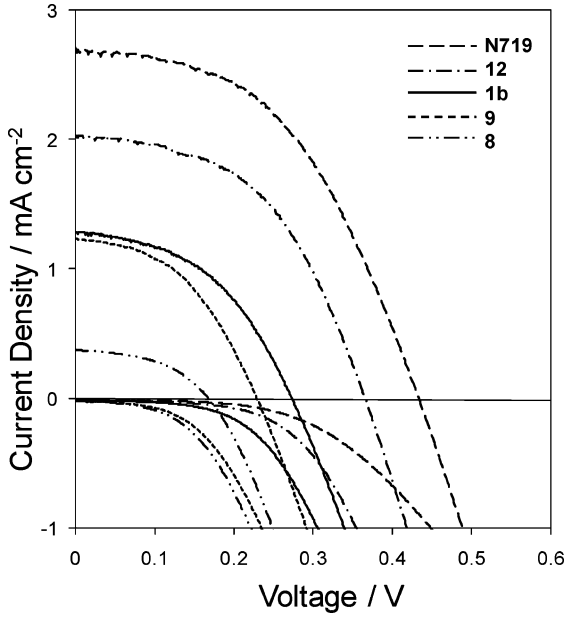

Figure 9. Typical illuminated and dark $J-V$ data for DSCs prepared with the sensitizing dyes anchored on TiO_2 films.

and reduces the number of molecules that can adhere to the TiO_2 surface. Among the dyads, **1b** had a slightly greater coverage than **1a**.

The phthalocyanine dyes **6**−**9** generally exhibited low coverage. Inclusion of peripheral *tert*-butyl groups on the macrocycle lead to a 1.7-fold decrease in surface density compared to the unsubstituted analogues. Surprisingly, complexes bearing 3,4-pyridinedicarboxylic acid axial ligands showed approximately twice the density of complexes with 4-pyridinecarboxylic acid ligands. It is apparent that while the PcRu-containing complexes absorb significantly more light than the BpyRu complexes, they are more bulky and far fewer molecules are adsorbed on a given area of TiO_2 surface.

DSC Performance. Figure 9 shows representative photocurrent-voltage curves (J vs V) collected for DSCs sensitized with dyes synthesized in this work. Data for the commercial DSC dye, N719, are also included for reference. Numerical $J-V$ data are collected in Table 2 together with the maximum power output (P_{max}), the fill factor, efficiency (η), and dye coverage. The DSCs and conditions used for testing allowed for ranking of various aspects of cell performance; however, the overall DSC efficiencies were not optimized in this study.

N719-sensitized DSCs performed significantly better than those prepared with the other sensitizing dyes. DSCs prepared using the monomeric phthalocyanine dyes **6**−**9** performed the poorest of the series. Inclusion of *tert*-butyl groups on the macrocycle periphery had an insignificant effect on cell performance. The use of 3,4-pyridinedicarboxylic acid as the anchoring ligand caused a three- to six-fold increase in V_{oc} and P_{max}, a trend previously noted for PcRu-based DSCs.[12] The superior performance of the **12**-sensitized DSCs compared to those sensitized with **1a** and **1b** indicates that inclusion of the metallophthalocyanine unit has a detrimental overall effect. While **1a** and **1b** gave indistinguishable V_{oc} data, **1b** yielded higher J_{sc} and P_{max} values.

The photovoltage of a DSC is related to the difference between the Fermi level of the TiO_2 under illumination and the redox potential of the mediating redox couple.[61] Sensitizing dyes in the series that contain PcRu units yielded lower V_{oc}'s than the complexes containing only a BpyRu center, a pattern which is consistent with previous reports of PcRu-based DSCs using an iodine/iodide redox mediator.[11−13] The decrease in V_{oc} has been attributed to an increase in the electron/electrolyte recombination rate catalyzed by the macrocycle.[12] The dark current characteristics of these cells (see Figure 9) show that the PcRu-based dyes accelerate recombination. The onset of the dark current, which corresponds to the transfer of electrons from the TiO_2 to I_2 (the recombination reaction), occurs at lower voltages where PcRu centers are present. Inclusion of the PcRu chromophores in the dyads failed to promote an increase in V_{oc} compared to that of **12** suggesting that if hole hopping and/or stepwise injection were occurring, any gain in V_{oc} was negated by PcRu-catalyzed recombination. The use of 4-*tert*-butylpyridine to suppress recombination was explored in cells sensitized with **9** and **1b**. In both cases substantial increases in V_{oc} were achieved; however, an accompanying decrease in cell current was observed and the overall power output of the cells decreased.

Despite the strong visible light absorption properties of the PcRu dyes at ~650 nm that make this class of complex appealing for DSC applications, low J_{sc}'s were obtained using **6**−**9**. Complexes **7** and **9**, which contained 3,4-pyridinedi-

(61) Kalyanasundaram, K.; Gratzel, M. *Coord. Chem. Rev.* **1998**, *177*, 347.

carboxylic acid as an anchoring ligand, gave superior photocurrent yields. This finding is consistent with other PcRu dyes bearing 4- and 3,4-pyridinedicarboxylic acid anchoring groups.[10−12] The increase in J_{sc} may at least in part be attributed to the higher surface density of dye afforded by using 3,4-pyridinedicarboxylic acid. The magnitude of the difference in J_{sc} also suggests that poor charge injection efficiency plays a role in the low current outputs of **6** and **8**.

Ranking the sensitizing dyes according to photocurrent generation *per molecule* (by dividing J_{sc} by the number of surface-adsorbed molecules) reveals that the dyads are superior photocurrent generators than N719, and that **9** is the most efficient dye. Inclusion of *tert*-butyl substituents on the phthalocyanine ring had little effect on cell performance; however, **8** and **9** were significantly better at current generation per molecule than **6** or **7**. This may be due to the ∼100 mV negative shift in the first ring based oxidation caused by the peripheral *tert*-butyl groups or the prevention of aggregation. The dyads performed better on a per molecule basis than **12**, suggesting that inclusion of the phthalocyanine chromophore, while detrimental to overall cell performance, did improve the ability of the molecule to generate current. **1b**, which showed a 20% improvement in the number of molecules absorbed to the TiO_2 surface compared to **1a**, had an 18% increase in J_{sc}.

These results highlight the importance of an often unreported aspect in sensitizing dye design, that of molecular size and thus dye coverage of electrode surfaces. Supramolecular systems and macromolecules can offer many attractive properties compared to smaller sensitizing dyes but the concurrent decrease in dye coverage may negate the positive effects.

Also, a sensitive method for measuring the number of surface-adsorbed dye molecules has been developed that utilizes ICP MS to determine the amount of dye desorbed from TiO_2 electrodes. With the common use of carboxyl anchoring groups, the method should be widely applicable for the measurement of dye coverage on electrode surfaces for many metal-based dyes used in DSCs.

Conclusions

Four ruthenium phthalocyanine complexes and two dyads consisting of ruthenium phthalocyanine and bis(bipyridyl)-ruthenium(II) chromophores bearing carboxyl functionality have been synthesized. The ruthenium phthalocyanine dyes display optical and redox properties typical for this class of complex, with minor variations due to axial ligand and peripheral substitution. The electrochemical investigation of the dyads indicated that both stepwise electron injection and hole hopping were energetically feasible processes. DSCs fabricated with the prepared dyes were less efficient than those fabricated using N719; however, on a per molecule basis the dyads and $[Bu_4N]_2[\{(t\text{-}Bu)_4Pc\}Ru\{3,4\text{-}py(COOH)COO^-\}_2]$ were superior photocurrent generators. The results indicate that the ability of dye molecules to densely populate TiO_2 electrode surfaces is a key feature in their success as sensitizing dyes. In terms of future directions, this finding should be considered by researchers when designing molecular dyes. As highlighted here, the importance of dye coverage in DSC performance suggests that there may often be a tradeoff between the ability of a dye to effectively absorb large amounts of light and inject electrons in the semiconductor and the size of molecule, which will in turn effect its coverage of the surface.

Experimental Section

Physical Measurements. ^{1}H NMR spectra were recorded using a BVT 3000 Bruker Spectrospin instrument operating at 300.13 MHz. Spectra are referenced internally to residual protic solvent ($CHCl_3$, δ 7.26 and DMSO δ 2.49). UV−visible spectra were recorded on an Agilent 8453 UV−visible spectrophotometer using dichloromethane as solvent. Infrared spectra were recorded using a Nicolet Magna IR-760 spectrometer with complexes dispersed in KBr discs. Electrospray ionization mass spectrometry (ESI-MS) was performed using a Perkin-Elmer SCIEX API300 Triple Quadrupole Mass Spectrometer. The general conditions were as follows: ion spray voltage = 5000V, drying gas temperature = 50 °C, orifice voltage = 30V, ring voltage = 340V, and injection via syringe pump. Spectra were averaged over 10 scans. Inductively coupled plasma mass spectrometry (ICP MS) were performed using an Agilent Technologies 7500ce instrument fitted with a "cs" lens system for improved sensitivity. A 4-point calibration curve for ^{100,101,104}Ru was constructed in the range of 1 ng kg^{-1} to 1 μg kg^{-1}. Correlation coefficients for each isotope were 1.000 with sub ng kg^{-1} detection limits. The conditions for ICP-MS analysis were as follows: RF power = 1600 W, sample depth = 9 mm, carrier gas flow 0.4 L min^{-1}, makeup gas flow 0.2 L min^{-1}, optional gas 21%, spray chamber temperature −5 °C, and helium reaction gas flow 4 mL min^{-1}. Elemental microanalyses were carried out by the Microanalytical Service Unit at the Research School of Chemistry, Australian National University. We note that difficulty in obtaining analyses agreeing to within 0.4% was encountered for several of the phthalocyanine-containing complexes, which may be due to incomplete combustion of the very stable RuPc unit.[9,43,62,63] Experimental conditions employed in cyclic voltammetry and spectroelectrochemical measurements are given elsewhere.[9]

Chemicals. $[PcRu(PhCN)_2]$,[64] $[\{(t\text{-}Bu)_4Pc\}Ru(PhCN)_2]$,[9] $[\{(t\text{-}Bu)_4Nc\}Ru(PhCN)_2]$,[65] *bis*(2-methylpropyl)-2,2′-bipyridine-4,4′-dicarboxylate (iBu$_2$dcbpy),[25] were prepared by literature procedures. 2,2′:4′,4″-Terpyridine was prepared by literature procedure[66] and purified using $Zn(NO_3)_2$.[67] The following were purchased commercially and used as received; ammonium thiocyanate (Ajax), tetra-*n*-butylammonium hydroxide (1 M solution in methanol, Aldrich), tetramethylammonium hydroxide (25 wt % in water, Aldrich), 4-*tert*-butylpyridine (Aldrich), $[RuCl_2(p\text{-cymene})]_2$ (Aldrich), 4-pyridinecarboxylic acid, 3,4-pyridinedicarboxylic acid (Aldrich), acetol (Aldrich), *N,N*-dicyclohexylcarbodiimide (Aldrich), 4-*N,N*-dimethylaminopyridine (Aldrich).

(62) Hanack, M.; Osio-Barcina, J.; Witke, E.; Pohmer, J. *Synthesis* **1992**, 211.
(63) Hanack, M.; Vermehren, P. *Chem. Ber.* **1991**, *124*, 1733.
(64) Bossard, G. E.; Abrams, M. J.; Darkes, M. C.; Vollano, J. F.; Brooks, R. C. *Inorg. Chem.* **1995**, *34*, 1524.
(65) Rawling, T.; McDonagh, A. M.; Colbran, S. B. *Inorg. Chim. Acta* **2008**, *361*, 49.
(66) Hayes, M. A.; Meckel, C.; Schatz, E.; Ward, M. D. *J. Chem. Soc., Dalton Trans.* **1992**, 703.
(67) Shen, Y.; Walters, K. A.; Abboud, K.; Schanze, K. S. *Inorg. Chim. Acta* **2000**, 300302, 414.

Syntheses. Preparation of (2-Oxopropyl)pyridine-4-carboxylate (4-pyCOOAce) and Bis(2-oxopropyl)pyridine-3,4-dicarboxylate (3,4-py(COOAce)$_2$). The same procedure was used to prepare 4-pyCOOAce and 3,4-py(COOAce)$_2$. The preparation of 4-pyCOOAce is given as an example. To dichloromethane (120 mL) at 0 °C was added 4-pyridinecarboxylic acid (800 mg, 6.5 mmol), acetol (577 mg, 7.8 mmol), *N,N*-dicyclohexylcarbodiimide (1.47 g, 7.1 mmol), and a catalytic amount of 4-*N,N*-dimethylaminopyridine (30 mg). The resulting suspension was stirred at 0 °C for an hour, then at room temperature for a further 4 days. Any remaining solid was filtered from the reaction mixture, and the dichloromethane was removed in vacuo. The crude product was then purified using silica column chromatography eluting with acetone: dichloromethane (1:1). A 912 mg quantity (78%) of (2-oxopropyl)pyridine-4-carboxylate was obtained as a waxy, low melting solid. Mp ∼ 25 °C. ^{1}H NMR (δ, 300 MHz, $CDCl_3$): 8.82 (d, J_{HH} = 5.4 Hz, 2H), 7.90 (d, J_{HH} = 4.2 Hz, 2H), 4.93 (s, 2H), 2.24 (s, 3H). MS (*m*/*z*): 179 ([M]$^+$), 149, 121, 106, 78, 51, 43.

3,4-py(COOAce)$_2$. White powder (yield 59%). An analytical sample was prepared by recrystallization using ethanol/water. Mp 86−87 °C. ^{1}H NMR (δ, 300 MHz, $CDCl_3$): 9.20 (d, J_{HH} = 0.6 Hz, 1H), 8.90 (d, J_{HH} = 5.1 Hz, 1H), 7.67 (dd, J_{HH} = 0.6, 5.1 Hz, 1H), 4.91 (s, 4H), 2.22 (s, 6H). MS (*m*/*z*): 280 ([M + H]$^+$), 249, 206, 150, 105, 79, 57, 43.

Preparation of [PcRu(4-pyCOOAce)$_2$]·3.5H$_2$O 2, and [PcRu{3,4-py(COOAce)$_2$}$_2$] 3. The same procedure was used to prepare **2** and **3**. The preparation of **2** is given as an example. To a deoxygenated dichloromethane solution (50 mL) of [PcRu(PhCN)$_2$] (200 mg, 0.24 mmol) was added 4-pyCOOAce (109 mg, 0.61 mmol). The resulting solution was heated at reflux for 3 h under a nitrogen atmosphere. The reaction mixture was then filtered and to the filtrate was added hexane (50 mL). The solution was left in the refrigerator at −3 °C for 16 h. The solid precipitate was collected by filtration, washed with hexane and air-dried. Yield 152 mg (64%) of a **2** as a blue solid.^{1}H NMR (δ, 300 MHz, $CDCl_3$): 9.18 (m, 8H), 7.92 (m, 8H), 5.81 (d, J_{HH} = 5.4 Hz, 4H), 4.26 (s, 4H), 2.54 (d, J_{HH} = 5.4 Hz, 4H), 1.78 (s, 6H). MS (*m*/*z*): 972 ([M + H]$^+$, 100). UV−vis (λ_{max}, nm [ε, 10^3 M^{-1} cm^{-1}]): 626 [63], 573sh, 461 [14], 371sh, 314 [103]. Anal. Calcd for $C_{50}H_{41}N_{10}O_{9.5}Ru$: C 58.02, H 3.99, N 13.53. Found: C 57.80, H 3.40, N 14.21.

3: Blue powder (yield 59%). ^{1}H NMR (δ, 300 MHz, $CDCl_3$): 9.18 (m, 8H), 7.94 (m, 8H), 5.60 (d, J_{HH} = 6.0 Hz, 2H), 4.26 (s, 4H), 4.18 (s, 4H), 2.91 (s, 2H), 2.60 (d, J_{HH} = 6.0 Hz, 2H), 2.06 (s, 6H), 1.79 (s, 6H). MS (*m*/*z*): 1172 ([M]$^+$, 100). UV−vis (λ_{max}, nm [ε, 10^3 M^{-1} cm^{-1}]): 635 [52], 583sh, 475 [11], 378sh, 312 [97]. Anal. Calcd for $C_{58}H_{42}N_{10}O_{12}Ru$: C 59.44, H 3.61, N 11.95. Found: C 59.11, H 3.76, N 12.01.

Preparation of [{(*t*-Bu)$_4$Pc}Ru(4-pyCOOAce)$_2$] 4 and [{(*t*-Bu)$_4$Pc}Ru{3,4-py(COOAce)$_2$}$_2$] 5. The same procedure was used to prepare **4** and **5**. The preparation of **4** is given as an example. To a deoxygenated dichloromethane solution (50 mL) of [{(*t*-Bu)$_4$Pc}Ru(PhCN)$_2$] (200 mg, 0.19 mmol) was added 4-pyCOOAce (86 mg, 0.48 mmol). The resulting solution was heated at reflux for 3 h under a nitrogen atmosphere. After cooling to room temperature the solvent was removed in vacuo. The crude product was purified by silica column chromatography eluting with dichloromethane/hexane (4:1) to yield 134 mg (59%) of a blue solid.^{1}H NMR (δ, 300 MHz, $CDCl_3$): 8.84 (m, 4H), 8.76 (m, 4H), 7.85 (m, 4H), 5.80 (d, J_{HH} = 6.6 Hz, 4H), 4.26 (s, 4H), 2.59 (d, J_{HH} = 6.6 Hz, 4H), 1.77 (s, 6H), 1.75 (s, 36H). MS (*m*/*z*): 1197 ([M + H]$^+$, 100). UV−vis (λ_{max}, nm [ε, 10^3 M^{-1} cm^{-1}]): 634 [61], 580sh, 471 [14], 370sh, 316 [112]. Anal. Calcd for $C_{66}H_{66}N_{10}O_6Ru$: C 66.26, H 5.56, N 11.71. Found: C 66.13, H 5.49, N 11.51.

5: Blue powder (yield 43%).^{1}H NMR (δ, 300 MHz, $CDCl_3$): 9.03 (m, 4H), 8.92 (m, 4H), 7.92 (m, 4H), 5.58 (d, J_{HH} = 6.0 Hz, 2H), 4.26 (s, 4H), 4.16 (s, 4H), 2.95 (s, 2H), 2.64 (d, J_{HH} = 6.0 Hz, 2H), 2.10 (s, 6H), 1.79 (s, 6H), 1.75 (s, 36H). MS (*m*/*z*): 1397 ([M]$^+$, 100). UV−vis (λ_{max}, nm [ε, 10^3 M^{-1} cm^{-1}]): 645 [70], 591sh, 481 [12], 379sh, 315 [117]. Anal. Calcd for $C_{74}H_{74}N_{10}O_{12}Ru$: C 63.64, H 5.34, N 10.03. Found: C 63.69, H 5.63, N 9.98.

Preparation of [Bu$_4$N]$_2$[PcRu(4-pyCOO$^-$)$_2$]·4.5H$_2$O 6 and [Bu$_4$N]$_2$[{(*t*-Bu)$_4$Pc}Ru(4-pyCOO$^-$)$_2$] 8. The same procedure was used to prepare **6** and **8** from the corresponding acetol-protected precursors. The preparation of **8** is given as an example. **4** (50 mg, 0.04 mmol) was dissolved in THF (5 mL) and 1 M tetra-*n*-butylammonium hydroxide solution (418 μL, 0.42 mmol) was added. The mixture was stirred for 20 m, after which the solvent was removed in vacuo. The residue was suspended in water (10 mL), and the solid collected by filtration. The solid was washed with water and air-dried to give 64 mg (97%) of **8** as a blue solid. ^{1}H NMR (δ, 300 MHz, $CDCl_3$): 9.15 (m, 4H), 9.01 (m, 4H), 7.90 (m, 4H), 5.72 (d, J_{HH} = 6.6 Hz, 4H), 2.73 (t, J_{HH} = 8.2 Hz, 16H), 2.45 (d, J_{HH} = 6.6 Hz, 4H), 1.72 (m, 36H), 1.14 (br, 16H), 0.96 (sextet, J_{HH} = 7.0 Hz, 16H), 0.65 (t, J_{HH} = 7.0 Hz, 24H). MS (*m*/*z*): 1105 ([M − 2{*n*-Bu$_4$N} + Na]$^-$, 100). UV−vis (λ_{max}, nm [ε, 10^3 M^{-1} cm^{-1}]): 629 [62], 576sh, 379sh, 317 [104]. Anal. Calcd for $C_{92}H_{137}N_{12}O_{8.5}Ru$: C 67.04, H 8.37, N 10.19. Found: C 66.99, H 7.65, N 9.92.

6: Blue solid (yield 92%). ^{1}H NMR (δ, 300 MHz, $CDCl_3$): 9.11 (m, 8H), 7.83 (m, 8H), 5.72 (d, J_{HH} = 6.6 Hz, 4H), 2.68 (t, J_{HH} = 8.2 Hz, 16H), 2.42 (d, J_{HH} = 6.6 Hz, 4H), 1.10 (br, 16H), 0.94 (sextet, J_{HH} = 7.0 Hz, 16H), 0.63 (t, J_{HH} = 7.0 Hz, 24H). UV−vis (λ_{max}, nm [ε, 10^3 M^{-1} cm^{-1}]): 623 [63], 571sh, 379sh, 316 [92]. MS (*m*/*z*): 858 ([M − 2{*n*-Bu$_4$N}]$^-$, 100). Anal. Calcd for $C_{76}H_{106}N_{12}O_9Ru$: C 63.71, H 7.45, N 11.73. Found: C 63.28, H 6.56, N 11.67.

Preparation of [Bu$_4$N]$_2$[PcRu{3,4-py(COOH)COO$^-$}$_2$] 7 and [Bu$_4$N]$_2$[{(*t*-Bu)$_4$Pc}Ru{3,4-py(COOH)COO$^-$}$_2$]·3H$_2$O 9. The same procedure was used to prepare **7** and **9** from the corresponding acetol-protected precursors. The preparation of **9** is given as an example. **5** (41 mg, 0.029 mmol) was dissolved in 1 M tetra-*n*-butylammonium hydroxide solution (5 mL) and stirred at room temperature for 20 min. The solvent was then removed in vacuo leaving a liquid residue which was dissolved in water (10 mL). The pH of the solution was adjusted to 6.3 using 0.1 M nitric acid, at which point precipitation occurred. The suspension was left in a refrigerator at −3 °C overnight, then the solid collected by filtration. A 44 mg quantity of **9** (90%) was collected as a blue powder. ^{1}H NMR (δ, 300 MHz, $CDCl_3$): 9.16 (m, 4H), 9.07 (m, 4H), 7.90 (m, 4H), 6.03 (d, J_{HH} = 6.0 Hz, 2H), 3.49 (s, 2H), 2.86 (t, J_{HH} = 8.2 Hz, 16H), 2.52 (d, J_{HH} = 6.0 Hz, 2H), 1.72 (m, 36H), 1.38 (br, 16H), 1.12 (sextet, J_{HH} = 7.0 Hz, 16H), 0.85 (t, J_{HH} = 7.0 Hz, 24H). UV−vis (λ_{max}, nm [ε, 10^3 M^{-1} cm^{-1}]): 629 [64], 576sh, 455 [12], 377sh, 317 [111]. MS (*m*/*z*): 1170 ([M − 2{*n*-Bu$_4$N} + H]$^-$, 100). Anal. Calcd for $C_{94}H_{134}N_{12}O_{11}Ru$: C 66.06, H 7.90, N 9.83. Found: C 66.29, H 7.38, N 9.47.

7: Blue powder (yield 86%). ^{1}H NMR (δ, 300 MHz, $CDCl_3$): 9.14 (m, 8H), 7.83 (m, 8H), 6.05 (d, J_{HH} = 6.3 Hz, 2H), 3.51 (s, 2H), 2.87 (t, J_{HH} = 8.2 Hz, 16H), 2.51 (d, J_{HH} = 6.0 Hz, 2H), 1.33 (br, 16H), 1.14 (sextet, J_{HH} = 7.0 Hz, 16H), 0.80 (t, J_{HH} = 7.0 Hz, 24H). UV−vis (λ_{max}, nm [ε, 10^3 M^{-1} cm^{-1}]): 624 [60], 571sh, 445 [10], 373sh, 316 [91]. MS (*m*/*z*): 947 ([M − 2{*n*-Bu$_4$N} + H]$^-$, 100). Anal. Calcd for $C_{78}H_{96}N_{12}O_8Ru$: C 65.48, H 6.76, N 11.75. Found: C 65.08, H 6.91, N 11.75.

Preparation of [Ru(*i*Bu$_2$dcbpy)(tpy)Cl$_2$] 10. [RuCl$_2$(*p*-cymene)]$_2$ (526 mg, 0.86 mmol) and *i*Bu$_2$dcbpy (612 mg, 1.72 mmol) were

dissolved in butanol (500 mL). The mixture was stirred at 85 °C for 1.5 h under nitrogen with the reaction vessel shielded from light. 2,2′:4′,4″-Terpyridine (400 mg, 1.72 mmol) was then added, and the resulting solution was heated at reflux for 2.5 h. The ethanol was removed in vacuo, and the crude complex purified by column chromatography eluting with methanol:dichloromethane (12:88). A 170 mg quantity (13%) of **10** was obtained as a black solid. ^{1}H NMR (δ, 300 MHz, $CDCl_3$): 10.55 (d, J_{HH} = 6.0 Hz, 1H of isomer a), 10.32 (d, J_{HH} = 6.0 Hz, 1H of isomer b), 10.22 (d, J_{HH} = 4.8 Hz, 1H of isomer b), 8.85−8.70 (m, Hs from isomers a and b), 8.64 (d, J_{HH} = 1.5 Hz, 1H of isomer a), 8.40 (m, 1H of isomer a), 8.28 (m, 1H of isomer a), 8.16 (dt, J_{HH} = 1.5, 6.0 Hz, 1H of isomer a), 7.88 (m, H of isomer a and b), 7.84 (d, J_{HH} = 6.0 Hz, 1H of isomer b), 7.79 (dd, J_{HH} = 1.8, 6.0 Hz, 1H of isomer b), 7.74 (d, J_{HH} = 6.0 Hz, 1H of isomer a), 7.63−7.47 (m, Hs of isomer a and b), 7.05 (dd, J_{HH} = 1.8, 6.0 Hz, 1H of isomer b), 6.90 ((t, J_{HH} = 6.0 Hz, 1H of isomer b), 4.29 (d, J_{HH} = 6.3 Hz, CH_2 of isomer a and b), 4.12 (d, J_{HH} = 6.6 Hz, CH_2 of isomer a and b), 2.21 (sep, J_{HH} = 6.6 Hz, CH of isomer a and b), 2.06 (sep, J_{HH} = 6.6 Hz, CH of isomer a and b), 1.11 (d, J_{HH} = 6.6 Hz, CH_3 of isomer a and b), 0.98 (d, J_{HH} = 6.6 Hz, CH_3 of isomer a and b). UV−vis (λ_{max}, nm [ε, 10^3 M^{-1} cm^{-1}]): 587 [12], 433 [12], 319 [26], 308 [31]. MS (*m*/*z*): 763 ([M + H]$^+$, 100).

Preparation of [Ru(*i*Bu$_2$dcbpy)(tpy)(NCS)$_2$] 11. To a deoxygenated solution of **10** (343 mg, 0.45 mmol) in ethanol (50 mL) was added [NH_4]NCS (1.372 g, 18.02 mmol). The reaction mixture was heated at reflux for 3 h under a nitrogen atmosphere. The ethanol was removed in vacuo, and the crude complex purified by column chromatography eluting with methanol/dichloromethane (7:93). A 228 mg quantity (63%) of **11** was obtained as a dark red solid. ^{1}H NMR (δ, 300 MHz, $CDCl_3$): 9.79 (d, J_{HH} = 5.7 Hz, 1H of isomer a), 9.59 (d, J_{HH} = 6.0 Hz, 1H of isomer b), 9.49 (d, J_{HH} = 4.5 Hz, 1H of isomer b), 8.87 (d, J_{HH} = 5.1 Hz, 1H of isomer a), 8.82 (d, J_{HH} = 6.0 Hz, 1H of isomer a), 8.78 (d, J_{HH} = 4.8 Hz, 1H of isomer a), 8.66 (s, 1H of isomer a), 8.39 (d, J_{HH} = 7.5 Hz, 1H of isomer b), 8.34 (d, J_{HH} = 1.5 Hz, 1H of isomer b), 8.27−8.20 (m, H of isomer a and b), 8.07 (td, J_{HH} = 1.2, 7.8 Hz, 1H of isomer b), 7.86 (dd, J_{HH} = 1.8, 5.7 Hz, 1H of isomer b), 7.77−7.67 (m, H of isomer a and b), 7.58 (dt, J_{HH} = 1.5, 6.0 Hz, 1H of isomer a), 7.49−7.44 (m, H of isomer a and b), 7.38 (d, J_{HH} = 5.7 Hz, 1H of isomer b), 7.15 (dd, J_{HH} = 1.8, 6.0 Hz, 1H of isomer b), 7.06 (t, J_{HH} = 6.0 Hz, 1H of isomer b), 4.32 (d, J_{HH} = 6.0 Hz, CH_2 of isomer a and b), 4.16 (d, J_{HH} = 6.6 Hz, CH_2 of isomer a and b), 2.23 (sep, J_{HH} = 6.6 Hz, CH of isomer a and b), 2.07 (sep, J_{HH} = 6.9 Hz, CH of isomer a and b), 1.12 (d, J_{HH} = 6.6 Hz, CH_3 of isomer a and b), 0.97 (d, J_{HH} = 6.6 Hz, CH_3 of isomer a and b). UV−vis (λ_{max}, nm [ε, 10^3 M^{-1} cm^{-1}]): 558 [12], 415 [12], 318 [30], 307 [34]. MS (*m*/*z*): 807 ([M]$^+$, 100). Anal. Calcd for $C_{37}H_{35}N_7O_4RuS_2$: C, 55.07; H, 4.37; N, 12.15. Found: C, 54.71; H, 4.46; N, 11.89.

Preparation of [(Bu_4N)$_{0.5}$] [Ru(dcbpy)(tpy)(NCS)$_2$]·2.5H$_2$O 12. **11** (26 mg, 0.032 mmol) was dissolved in 1 M tetra-*n*-butylammonium hydroxide solution (7 mL) and stirred at room temperature for 20 min. The solvent was then removed in vacuo leaving a liquid residue which was dissolved in water (10 mL). The pH of the solution was adjusted to 3.9 using 0.1 M nitric acid, at which point precipitation occurred. The suspension was left in a refrigerator at −3 °C overnight, then the solid collected by filtration to yield 22 mg (85%) of the desired compound. ^{1}H NMR (δ, 300 MHz, DMSO-d_6): 9.38 (m, H of isomer a and b), 9.28 (d, J_{HH} = 5.1 Hz, 1H of isomer b), 9.18 (s, 1H of isomer b), 9.09 (s, 1H of isomer a), 9.05 (d, J_{HH} = 7.5 Hz, 1H of isomer a), 8.99 (s, 1H of isomer b), 8.94−8.83 (m, H of isomer a and b), 8.72 (br, 1H of isomer a), 8.45 (dd, J_{HH} = 1.8, 6.0 Hz, 1H of isomer b), 8.34−2.69 (m, H of isomer a and b), 8.05−7.85 (m, H of isomer a and b), 7.81 (d, J_{HH} = 5.7 Hz, 1H of isomer b), 7.72 (d, J_{HH} = 5.7 Hz, 1H of isomer b), 7.63−7.53 (m, H of isomer a and b), 7.27 (t, J_{HH} = 6.6 Hz, 1H of isomer b), 3.15 (t, J_{HH} = 8.4 Hz, CH_2 of TBA), 1.53 (pent, J_{HH} = 7.5 Hz, CH_2 of TBA), 1.29 (sextet, J_{HH} = 7.2 Hz, CH_2 of TBA), 0.83 (t, J_{HH} = 7.2 Hz, CH_3 of TBA). UV−vis (λ_{max}, nm [ε, 10^3 M^{-1} cm^{-1}]): 522 [13], 384 [11], 308 [38]. MS (*m*/*z*): 694 ([M − 0.5{*n*-Bu_4N}]$^-$, 100). Anal. Calcd for $C_{37}H_{41}N_{7.5}O_{6.5}S_2Ru$: C 51.68, H 4.81, N 12.22. Found: C 51.60, H 4.13, N 12.38.

Preparation of 13a and 13b. [{(*t*-Bu)$_4$Pc}Ru(PhCN)$_2$] (216 mg, 0.21 mmol), 4-*tert*-butylpyridine (31 mg, 0.23 mmol), and **11** (184 mg, 0.23 mmol) were dissolved in deoxygenated dichloromethane (50 mL). The resulting solution was heated at reflux for 3.5 h under a nitrogen atmosphere. The dichloromethane was removed in vacuo, and the crude products were purified by column chromatography eluting with ethyl acetate/dichloromethane (1:19). **13a:** Yield 30 mg (8%) as a blue solid. ^{1}H NMR (δ, 300 MHz, $CDCl_3$): 9.61 (d, J_{HH} = 6.0 Hz, 1H, *g*), 9.24 (m, 4H, *aa*), 9.13 (m, 5H, *cc* and *s*), 8.69 (d, J_{HH} = 1.5 Hz, 1H, *i*), 8.52 (d, J_{HH} = 1.5 Hz, 1H, *j*), 8.11 (dd, J_{HH} = 1.5, 6.0 Hz, 1H, *h*), 7.99 (m, 4H, *bb*), 7.57 (d, J_{HH} = 7.5 Hz, 1H, *p*), 7.48 (d, J_{HH} = 8.1 Hz, 1H, *o*), 7.33 (dd, J_{HH} = 1.5, 6.0 Hz, 1H, *k*), 7.25 (m, 1H, *l*), 7.20 (d, J_{HH} = 6.0 Hz, 1H, *m*), 7.09 (d, J_{HH} = 1.5 Hz, 1H, *q*), 6.89 (d, J_{HH} = 5.4 Hz, 1H, *n*), 6.79 (dd, J_{HH} = 1.8, 6.0 Hz, 1H, *r*), 5.57 (d, J_{HH} = 6.9 Hz, 2H, *t* and *u*), 5.22 (d, J_{HH} = 7.2 Hz, 2H, *ff*), 4.24 (d, J_{HH} = 5.7 Hz, 2H, *f*), 4.07 (d, J_{HH} = 6.6 Hz, 2H, *c*), 2.70 (d, J_{HH} = 6.9 Hz, 2H, *v* and *w*), 2.40 (d, J_{HH} = 6.9 Hz, 2H, *ee*), 2.15 (sep, J_{HH} = 6.6 Hz, 1H, *e*), 1.98 (sep, J_{HH} = 6.6 Hz, 1H, *b*), 1.76 (m, 36H, *dd*), 1.05 (d, J_{HH} = 6.6 Hz, 6H, *d*), 0.92 (d, J_{HH} = 6.6 Hz, 6H, *a*), 0.34 (s, 9H, *gg*). UV−vis (λ_{max}, nm [ε, 10^3 M^{-1} cm^{-1}]): 629 [70], 576sh, 371sh, 318 [142]. MS (*m*/*z*): 1782 ([M + 2H]$^+$, 100). Anal. Calcd for $C_{94}H_{96}N_{16}O_4Ru_2S_2$: C 63.42, H 5.44, N 12.59. Found: C 63.93, H 5.62, N 12.12.

13b·2H$_2$O. Yield 24 mg (6%) as a blue solid. ^{1}H NMR (δ, 300 MHz, $CDCl_3$): 9.54 (d, J_{HH} = 5.7 Hz, 1H, *g*), 9.35 (d, J_{HH} = 5.4 Hz, 1H, *m*), 9.20 (m, 4H, *aa*), 9.08 (m, 4H, *cc*), 8.64 (d, J_{HH} = 1.2 Hz, 1H, *i*), 8.49 (d, J_{HH} = 1.2 Hz, 1H, *j*), 8.05 (dd, J_{HH} = 1.7, 6.0 Hz, 1H, *h*), 7.98 (m, 4H, *bb*), 7.82 (td, J_{HH} = 1.5, 8.1 Hz, 1H, *o*), 7.68 (d, J_{HH} = 7.8 Hz, 1H, *p*), 7.59 (td, J_{HH} = 1.2, 6.3 Hz, 1H, *n*), 7.39 (m, 2H, *k* and *l*), 7.02 (d, J_{HH} = 1.2 Hz, 1H, *q*), 6.98 (d, J_{HH} = 6.0 Hz, 1H, *s*), 6.02 (dd, J_{HH} = 1.8, 6.0 Hz, 1H, *r*), 5.29 (d, J_{HH} = 6.9 Hz, 2H, *t* and *u*), 5.19 (d, J_{HH} = 5.7 Hz, 2H, *ff*), 4.22 (d, J_{HH} = 6.8 Hz, 2H, *f*), 4.06 (d, J_{HH} = 6.3 Hz, 2H, *c*), 2.58 (d, J_{HH} = 6.9 Hz, 2H, *v* and *w*), 2.35 (d, J_{HH} = 6.9 Hz, 2H, *ee*), 2.14 (sep, J_{HH} = 6.6 Hz, 1H, *e*), 1.98 (sep, J_{HH} = 6.6 Hz, 1H, *b*), 1.73 (m, 36H, *dd*), 1.04 (d, J_{HH} = 6.9 Hz, 6H, *d*), 0.92 (d, J_{HH} = 6.6 Hz, 6H, *a*), 0.32 (s, 9H, *gg*). UV−vis (λ_{max}, nm [ε, 10^3 M^{-1} cm^{-1}]): 629 [74], 575sh, 370sh, 317 [143]. MS (*m*/*z*): 1780 ([M]$^+$, 100). Anal. Calcd for $C_{94}H_{100}N_{16}O_6S_2Ru_2$: C 62.17, H 5.55, N 12.34. Found: C 62.43, H 5.39, N 12.17.

Preparation of 1a·4.5H$_2$O and 1b·5H$_2$O. The same procedure was used to prepare complexes **1a** and **1b**. The preparation of **1a** is given as an example. **13a** (22 mg, 0.012 mmol) was dissolved in 1 M tetra-*n*-butylammonium hydroxide solution (6 mL) and stirred at room temperature for 20 min. The solvent was then removed in vacuo leaving a liquid residue which was partitioned between water (20 mL) and diethyl ether (25 mL). The solid was collected by filtration and dried in vacuo, affording 23 mg (87%) of **1a** as a blue solid. ^{1}H NMR (δ, 300 MHz, $CDCl_3$): 9.23 (m, 4H, *aa*), 9.12 (m, 6H, *cc*, *s* and *g*), 8.88 (br, 1H, *i*), 8.67 (br, 1H, *j*), 8.17 (d, J_{HH} = 5.4 Hz, 1H, *h*), 7.98 (m, 4H, *bb*), 7.50 (d, J_{HH} = 7.8 Hz, 1H, *p*), 7.39 (m, 2H, *o* and *k*), 7.21 (d, J_{HH} = 5.7 Hz, 1H, *m*), 7.16 (s, 1H, *q*), 6.88 (m, 2H, *n* and *l*), 6.68 (dd, J_{HH} = 1.5, 6.3, Hz,

1H, *r*), 5.58 (d, J_{HH} = 6.9 Hz, 2H, *t* and *u*), 5.21 (d, J_{HH} = 7.2 Hz, 2H, *ff*), 3.20 (t, J_{HH} = 7.6 Hz, 16H), 2.69 (d, J_{HH} = 6.9 Hz, 2H, *v* and *w*), 2.41 (d, J_{HH} = 6.9 Hz, 2H, *ee*), 1.75 (m, 36H, *dd*), 1.57 (br, 16H), 1.29 (sextet, J_{HH} = 7.2 Hz, 16H), 0.83 (t, J_{HH} = 7.2 Hz, 24H), 0.33 (s, 9H, *gg*). UV−vis (λ_{max}, nm [ε, 10^3 M^{-1} cm^{-1}]): 630 [65], 575sh, 371sh, 313 [127]. MS (*m*/*z*): 1668 ([M − 2{*n*-Bu_4N}]$^-$, 100). Anal. Calcd for $C_{118}H_{159}N_{18}O_{8.5}S_2Ru_2$: C 63.50, H 7.18, N 11.30. Found: C 63.67, H 7.01, N 10.22.

1b: Blue powder (yield 93%). ^{1}H NMR (δ, 300 MHz, $CDCl_3$): 9.31 (d, J_{HH} = 5.1 Hz, 1H, *m*), 9.18 (m, 4H, *aa*), 9.06 (m, 5H, *cc* and *g*), 8.79 (s, 1H, *i*), 8.61 (s, 1H, *j*), 8.09 (d, J_{HH} = 5.1 Hz, 1H, *h*), 7.95 (m, 4H, *bb*), 7.74 (d, J_{HH} = 7.8 Hz, 1H, *o*), 7.65 (d, J_{HH} = 7.5 Hz, 1H, *p*), 7.49 (t, J_{HH} = 6.0 Hz, 1H, *n*), 7.44 (d, J_{HH} = 5.4 Hz, 1H, *k*), 6.99 (m, 3H, *q*, *s*, and *l*), 6.03 (d, J_{HH} = 6.0 Hz, 1H, *r*), 5.33 (d, J_{HH} = 6.6 Hz, 2H, *t* and *u*), 5.17 (d, J_{HH} = 6.9 Hz, 2H, *ff*), 3.22 (d, J_{HH} = 7.7 Hz, 16H), 2.57 (d, J_{HH} = 6.6 Hz, 2H, *v* and *w*), 2.36 (d, J_{HH} = 6.9 Hz, 2H, *ee*), 1.72 (m, 36H), 1.59 (br, 16H), 1.26 (sextet, J_{HH} = 7.2 Hz, 16H), 0.85 (t, J_{HH} = 7.2 Hz, 24H), 0.31 (s, 9H, *gg*). UV−vis (λ_{max}, nm [ε, 10^3 M^{-1} cm^{-1}]): 630 [69], 576sh, 472 [17], 371sh, 313 [130]. Anal. Calcd for $C_{118}H_{160}N_{18}O_9S_2Ru_2$: C 63.25, H 7.20, N 11.25. Found: C 62.93, H 6.73, N 11.09.

DSC Fabrication and Characterization. TiO_2 electrodes were prepared from Opaque Titania Working Electrodes (Dyesol Ltd.). Prior to absorption of the sensitizing dye the electrodes were heated at 450 °C for 40 min. When the electrodes cooled to 80 °C they were immersed in a 0.3 mM ethanol solution of the sensitizing dye for 24 h in the dark. The electrodes were then briefly sonicated in ethanol, thoroughly rinsed with more ethanol, and dried under a stream of nitrogen gas. In the case of $[Bu_4N]_{0.5}$[Ru(dcbpy)(tpy)$(NCS)_2$] **12** DMF was used as solvent. The cleaning procedure consisted of brief sonication in DMF and then ethanol, followed by soaking in ethanol for 5 h to remove the DMF. Cleaned electrodes were used immediately for photovoltaic measurements.

DSCs were fabricated by sandwiching the electrolyte solution between the freshly prepared dye coated TiO_2 working electrode and a Platinum Counter Electrode (Dyesol Ltd.). In all cases a Parafilm spacer was used between the electrodes. The electrolyte solution consisted of 0.05 M I_2 and 0.7 M LiI in 3-methoxypropionitrile. For measurements where 4-*tert*-butylpyridine was added to the electrolyte a concentration of 0.5 M was used. Photovoltaic data was measured using a 500 W halogen lamp giving 500 W/m^2 at the surface of the test cell (see Supporting Information for the lamp emission spectrum). The light intensity was measured using a Solar Light Co Thermopile. Current−voltage characteristics of the cells were measured by biasing the cells externally using an eDAQ e-chorder 401 potentiostat and recording the resulting photocurrent. Photovoltaic cells containing the various dyes were tested in triplicate.

Dye Coverage Measurements. Dye-coated TiO_2 electrodes were prepared and washed as described above. To ensure complete removal of unabsorbed dye molecules from the TiO_2 the electrodes were immersed in 3-methoxypropionitrile for 2 min, then rinsed again with ethanol and dried thoroughly under a stream of nitrogen. The dye-coated TiO_2 was then scraped off the electrodes and weighed into polypropylene vials. One milliliter of a 1 M tetramethylammonium hydroxide solution (ethanol/water, 7:3) was added, and desorption was allowed to occur for 2 h. The solutions were diluted to a known mass (∼5 g) using ethanol/water (7:3), and centrifuged at 4000 rpm for 3 min. The ICP-MS conditions were optimized on a 1 ppb tune solution in ethanol/water (7:3). The addition of oxygen to the carrier gas, low sample uptake rate, cooled spray chamber, and high plasma power were used to ensure complete combustion of the sample in the high carbon matrix.[68] Standards were prepared from a 1000 μg mL^{-1} Ru solution in dilute HCl (Ultra Scientific, U.S.A.), 1 mL of 1 M TMAOH in ethanol/water (7:3) and made to volume with ethanol/water (7:3) in polypropylene vials. An ethanol/water (7:3) solution was used to rinse the ICP-MS pump tubing between samples until background levels were reached to ensure no carry-over affected subsequent samples. Each dye was tested in duplicate.

Supporting Information Available: Further details are given in Figures S1−S19. This material is available free of charge via the Internet at http://pubs.acs.org.

IC802087N

(68) Dressler, V. L.; Pozebon, D.; Curtius, A. J. *Anal. Chim. Acta* **1999**, *379*, 175.